



Modeling the shear behavior of rock joints under various normal conditions

Shuilin Wang, Mingwei Guo, Guanhua Sun, Sujin Liu
State Key laboratory of Geomechanics and Geotechnical Engineering,
Institute of Rock and Soil Mechanics, Chinese Academy of Sciences,
Wuhan 430071, P. R. China

Changren Ke
School of Civil Engineering, Hubei University of Technology,
Wuhan 430068, P. R. China

ABSTRACT

The shear behavior of joints is studied under constant normal load (CNL), constant normal stiffness (CNS) and constant normal displacement (CND) conditions on the basis of the formerly proposed approach, in which the post-peak part of the shear stress-displacement curve is simulated in a stepwise manner. Strength softening and strength hardening processes are modeled in a unified form. Shear stress-displacement curves, dilation-shear displacement curves and normal stress-shear displacement curves are determined by the numerical method. They are compared with those published data under low normal stress and normal stiffness conditions, good agreements are observed. Shear stress-displacement curves, dilation-shear displacement curves and normal stress-shear displacement curves under high CNS and CND conditions are presented and analyzed. With the consideration of high cost in shear test under high CNS conditions, this study under high CNS and CND conditions can be taken as the improvement with respect to the study with low normal stress and normal stiffness conditions, which can bring insight into the deep underground engineering.

RÉSUMÉ

Le comportement du cisaillement du joint est étudié sous des conditions de charge normale constante (CNC), de rigidité normale constante (RNC) et de déplacement normal constant (DNC) sur la base de l'approche précédemment proposée, dans laquelle le cisaillement post-pic contrainte-déplacement courbe est simulée par paliers. Les processus de ramollissement et de durcissement sont modélisés sous une forme unifiée. Les courbes contrainte-déplacement de cisaillement, et de déplacement de dilatation-cisaillement et les celles normales de déplacement contrainte-cisaillement sont déterminées numériquement. Ils sont comparés avec les données publiées dans des conditions de faible contrainte normale et de rigidité normale, et de bons accords sont observés. Les courbes contrainte-déplacement de cisaillement, et de déplacement dilatation-cisaillement et les normales de déplacement contrainte-cisaillement dans des conditions CNC et RNC élevées sont présentées et analysées. Compte tenu du coût élevé du test de cisaillement sous des conditions CNC élevées, cette étude sous des conditions élevées de CNC et DNC peut être considérée comme une amélioration par rapport à l'étude avec des conditions de stress normal et de rigidité normale, ce qui peut apporter un aperçu dans l'ingénierie souterraine profonde.

1 INTRODUCTION

Joints or fractures have dramatic influences on the mechanical behavior of rock mass, and rational evaluation of the shear behavior is important in geotechnical engineering. Conventional direct shear tests in the laboratory or in situ are performed under constant normal load (CNL) condition in the past. Figure 1 shows the typical shear force-shear displacement and normal displacement-shear displacement curves obtained under CNL condition (Brady et al. 2004). The peak strength is reached after a small shear displacement and the residual strength is finally followed. The shear force-shear displacement curve is displayed in strength-softening mode. Meanwhile, shear dilation is observed.

However, the dilation caused by shear would probably be inhibited by the surrounding rock mass in underground caverns, especially at great depth. In these situations, the mode of shearing is close to constant normal stiffness (CNS) condition.

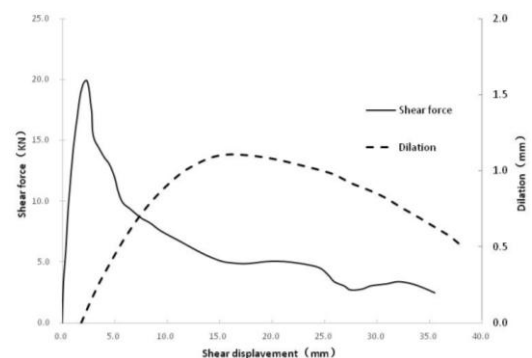


Figure 1. Shear force-shear displacement curve and normal displacement-shear displacement under CNL condition.

Typical shear stress-shear displacement and normal displacement-shear displacement curves under CNS

condition are shown in Figure 2 (adapted from Lee et al. 2014).

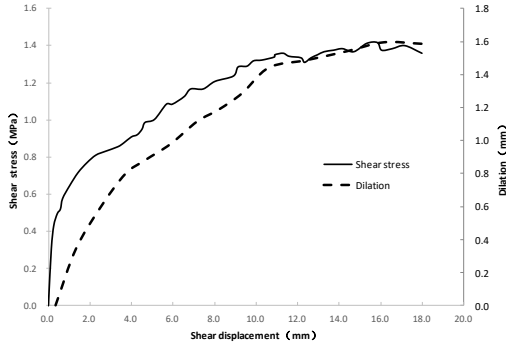


Figure 2. Shear stress-shear displacement curve and normal displacement-shear displacement under CNS condition.

Under CNS condition, the dilation is inhibited by the normal spring, the normal stress will increase during shear process. The shear stress-shear displacement curve is displayed in complicated modes. Sometimes it behaves in strength-hardening mode, whereas, sometimes it belongs to strength-softening mode. It depends on the initial normal stress and normal stiffness of the spring that are applied on the joint specimen.

With the consideration of complicated modes in shear stress-shear displacement curve under CNS conditions, a formerly proposed approach (Wang et al, 2011, 2016), in which the strength softening is simulated in a stepwise manner, is extended. The new approach for modeling strength softening and strength hardening process in a unified form is proposed, which efficiently simulate the shear behavior of rock joint. Shear stress-displacement curves, normal displacement-shear displacement curves and normal stress-displacement curves are obtained. The predicted results are compared with those published test data and good agreements are observed. Moreover, the shear stress-displacement curves, dilation-shear displacement curves and normal stress-displacement curves under high CNS and CND conditions are studied, as well.

2 FUNDAMENTAL CONSTITUTIVE EQUATIONS

There are two types of constitutive models. One is formulated by empirical method (Goodman et al 1968, Bandis et al 1983, Lee et al. 2014) and the other formulated by theoretical method (Plesha 1987, Ohnishi et al 1996, Wang et al 2003). The latter is derived based on the plasticity theory and it is used in the paper.

When irrecoverable deformation occurs, the shear displacement is decomposed into elastic and plastic parts. i.e.

$$du_i = du_i^e + du_i^p \quad [1]$$

The elastic part of the incremental displacements and the incremental stresses can be formulated by

$$d\sigma_i = k_{ij} du_j^e \quad [2]$$

where du_i is the incremental form of displacement, $d\sigma_i$ is the incremental form of stress, k_{ij} is the stiffness tensor, $i, j = n, t$ ('n' denotes the normal direction of the joint surface, and 't' denotes the tangential direction), superscripts 'e' and 'p' denote the elastic and plastic portion of the displacement, respectively.

The irrecoverable displacement is described by a flowing rule

$$du_i^p = d\lambda \frac{\partial Q}{\partial \sigma_i} \quad \text{when } F=0 \quad [3]$$

$d\lambda$ is a constant termed plastic multiplier. Q is the plastic potential corresponding to the yield function F . $d\lambda = 0$ when $F < 0$, and $d\lambda > 0$ when $F = 0$.

Eqs 1, 2 and 3 are combined to give the constitutive relation of joint model.

$$d\sigma_i = \left(k_{ij} - \frac{k_{ik} \partial Q / \partial \sigma_k \partial F / \partial \sigma_l \partial \sigma_j}{A + \partial F / \partial \sigma_m k_{mn} \partial Q / \partial \sigma_n} \right) du_j \quad [4]$$

Standard index notation is employed in which summation is implied on repeated indices (k, l, m and n).

$A (= d\sigma_i / du_i^p)$ is a scalar, with $A < 0$ for shear-softening

behavior, $A > 0$ for shear-hardening behavior, and $A = 0$ for perfectly plastic behavior.

Denote $k_{ij}^{ep} = k_{ij} - \frac{k_{ik} \partial Q / \partial \sigma_k \partial F / \partial \sigma_l \partial \sigma_j}{A + \partial F / \partial \sigma_m k_{mn} \partial Q / \partial \sigma_n}$, Eq. 4 can be written as

$$d\sigma_i = k^{ep}_{ij} du_j \quad [5]$$

Usually, k_{ij} is a positive definite matrix. Therefore, $\partial F / \partial \sigma_m k_{mn} \partial Q / \partial \sigma_n > 0$. When shear-softening behavior ($A < 0$) is considered, $A + \partial F / \partial \sigma_m k_{mn} \partial Q / \partial \sigma_n$ may be equal to zero. k^{ep}_{ij} is meaningless in this case. That is the reason why numerical solution for shear-softening problems is sometimes unstable.

Here Mohr–Coulomb criterion is used. The yield function is

$$F = \sigma_t - (c + \sigma_n \tan \phi) = 0 \quad [6]$$

and the plastic potential

$$Q = \sigma_t - (c + \sigma_n \tan \psi) \quad [7]$$

where c is cohesion, ϕ is friction angle and ψ is dilatancy angle.

3 THE APPROACH FOR MODELING THE SHEAR BEHAVIOR UNDER CNS CONDITION

3.1 Description of CNS shear test

The normal load is kept constant in conventional direct shear tests. But, in shear test under CNS condition (Indraratna et al. 1998, Jiang et al. 2004, Lee et al. 2014), springs are set in the normal direction of joint specimen. Dilation appears during the shearing process and this results in an increase in normal stress. In return, the increased normal stress will inhibit the dilation. Therefore, the shear behavior is much more complicated in CNS shear test than in conventional direct shear test.

The normal stress was calculated by the following equation.

$$\sigma_n = \sigma_{n0} + k_{n0}u_n \quad [8]$$

where σ_{n0} is the initial normal stress, k_{n0} the normal stiffness of the spring.

The incremental form of Eq. 8 is

$$\Delta \sigma_n = k_{n0} \Delta u_n \quad [9]$$

The increment of the normal stress is obtained by Eq. 9 during shear process under CNS condition.

3.2 Strength softening and strength hardening behavior and its modeling

In Figure 1, a peak point of shear stress appears in the early stage of the shear stress-displacement curve under the CNL condition, and then the residual part follows while shear deformation accrues. The peak point indicates the peak shear strength taken by the joint, and the residual part means the residual shear strength. The shear stress-shear displacement curve in Figure 1 demonstrates the strength softening mode of the joint. Meanwhile, the joint dilatancy accompanies the post peak part of the curve.

However, the shear stress-shear displacement curve displays the strength hardening mode under certain CNS condition as shown in Figure 2.

The actual observations show that the shear stress-shear displacement curve displays multiple shear modes of the joint. So, the joint could have completely different shear behavior during the shear process under CNS condition.

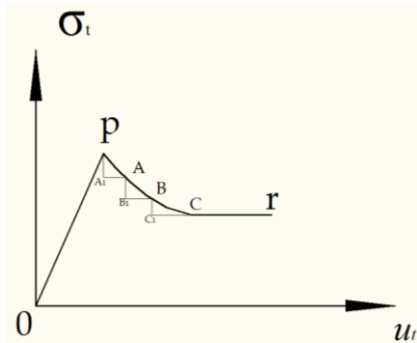


Figure 3 Idealized shear stress-displacement curve and a schematic diagram for modeling strength softening process of rock joints

For strength softening mode, idealized shear stress-shear displacement curve is depicted in Figure 3, which consists mostly of linear part 'op', strength softening part 'pc' and residual part 'cr'.

The shear stress-displacement curve in strength softening stage is usually nonlinear. The piecewise linear approximation is made when numerical analysis is performed under the framework of the classical theory of plasticity. Figure 3 shows that curve 'pc' is replaced by several piecewise linear segments and each segment usually has different negative slope. The piecewise linear segments are further treated in a stepwise manner.

For example, the strength softening segment 'AB' is simplified to be stress drop part 'AB₁' and plastic flow part 'B₁B'. Therefore, strength softening process from 'A' to 'B' becomes brittle-plastic one from 'A' to 'B₁' and then from 'B₁' to 'B'. The simplification can be made for the other segments in the same way. Instead of solving strength softening problem with negative slope, a series of brittle-plastic process can be effectively used to model strength softening behavior.

As shown in Figure 3, stress increment ($\Delta \sigma_i$) in segment AB consists of stress drop increment ($\Delta \sigma_i^d$) and plastic stress increment ($\Delta \sigma_i^f$). i.e.

$$\Delta \sigma_i = \Delta \sigma_i^d + \Delta \sigma_i^f \quad [10]$$

$\Delta \sigma_i^d$ can be determined by stresses in yield surfaces corresponding to point 'A' and 'B'. When Mohr-Coulomb criterion is considered,

$$\Delta \sigma_i^d = c_{(A)} + \sigma_{n(A)} \tan \varphi_{(A)} - c_{(B)} - \sigma_{n(B)} \tan \varphi_{(B)}$$

Subscripts 'A' and 'B' in parentheses indicate that strength parameters take the corresponding values in the load increments.

$$\Delta \sigma_i^f \text{ will be obtained by Eq. 4. } \Delta \sigma_i^f = k_{ij}^{ep} \Delta u_j$$

It should be noted that A equals to 0 in k_{ij}^{ep} .

For strength hardening mode, idealized shear stress-shear displacement curve is depicted in Figure 4, which consists of linear part 'op', strength hardening part 'pc' and 'cr'.

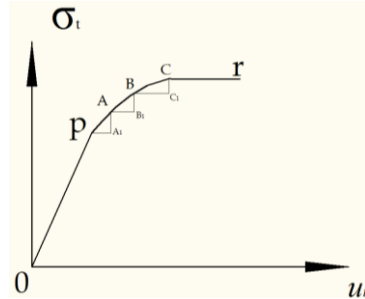


Figure 4 Idealized shear stress-displacement curve and a schematic diagram for modeling strength hardening process of rock joints

The shear stress-displacement curve in strength hardening stage is usually nonlinear. The piecewise linear approximation is made. Figure 4 shows that curve 'pc' is replaced by several piecewise linear segments and that the piecewise linear segments are further treated in a stepwise manner.

For example, the strength hardening segment 'AB' is simplified to be plastic flow part 'AB₁' and stress jump part 'B₁B'. Therefore, strength hardening process from 'A' to 'B' becomes plastic flow from 'A' to 'B₁' and then stress jump from 'B₁' to 'B'. The simplification can be made for the other segments in the same way.

Instead of solving strength hardening problem directly, a series of stress jump and plastic flow process can be utilized to model strength hardening behavior.

Stress increment ($\Delta\sigma_i$) in segment AB in Figure 4 consists of stress jump increment ($\Delta\sigma_i^d$) and plastic stress increment ($\Delta\sigma_i^f$). It has the same formulation as in Eq. [10]. But it should be noted that there is sign difference in $\Delta\sigma_i^d$ when strength softening and strength hardening are considered respectively.

3.3 Evolution of strength parameters

During shear process, strength parameters change from peak value to residual value as shown in Figure 5.

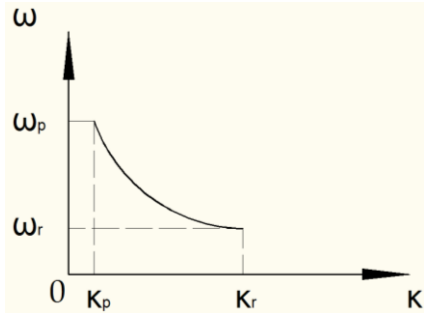


Figure 5 Schematic diagram for evolution of strength parameters

Suppose that the evolution of parameters is described by parabolic functions:

$$\omega(\kappa) = \begin{cases} a_1\kappa^2 + a_2\kappa + a_3 & \kappa_p \leq \kappa \leq \kappa_r \\ \omega_r & \kappa \geq \kappa_r \end{cases} \quad [11]$$

In Eq. 11, ω can represent any one of the strength parameters, such as c , ϕ and ψ . κ denotes the shear displacement. κ_p and κ_r correspond to the shear displacements when peak and residual strength appears. a_1 , a_2 and a_3 can be determined if the parabola passes

the coordinates (κ_p, ω_p) and (κ_r, ω_r) . In addition, the first-order derivative is zero at (κ_r, ω_r) .

3.4 The relationship among CNL, CNS and CND

The CNL condition can be represented by the CNS condition where the normal stiffness is zero, and the CND condition can also be represented by the CNS condition where the normal stiffness is large enough. i.e., CNL and CND conditions are the special cases of CNS condition.

4 APPLICATION OF THE PROPOSED APPROACH

4.1 Modeling the shear behavior of rock joints under CNS condition

According to the suggested method, a set of parameters from Lee et al. (2014) is used. Table 1 summarizes the properties of the joints. The initial normal stress $\sigma_{n0}=0.2\text{MPa}$, and various level of normal stiffness k_{n0} ($=0, 0.1, 0.5, 1.0$ and 1.5GPa/m) is considered.

Table 1. Parameters of the rock joint

Parameters	value
k_{ss} (GPa/m)	1.04
k_{nn} (GPa/m)	10.4
c_p (MPa)	0.3
ϕ_p (deg)	47.72
ψ_p (deg)	23.86
c_r (MPa)	0.1
ϕ_r (deg)	26.57
ψ_r (deg)	13.29
κ_p (mm)	0.5
κ_r (mm)	7.0

Figure 6 shows the shear behavior of the joint corresponding to the parameters in Table 1. Different shear behaviors of the joint are obtained by various k_{n0} . More importantly, test results (with '#') are compared with those obtained by proposed approach. It can be concluded that the predictions of the shear behaviors are in good agreement with the test results in most cases.

Test results show that the shear stresses will keep constant when $u_t > 14\text{mm}$. It is speculated that the residual dilatancy angle of the joint changes into 0.0° when $u_t = 14\text{mm}$. Therefore, ψ_r is assumed to be 0.0° when $u_t > 14\text{mm}$.

In Figure 6(a), the shear stress-displacement curves display a strength softening mode when $k_{n0} = 0$ or 0.1GPa/m , whereas the shear stress-displacement curves demonstrate a strength hardening mode when $k_{n0} \geq 0.5\text{GPa/m}$. In essence, whether the strength

softening or strength hardening mode appears depends on the combination of initial normal stress and normal spring stiffness.

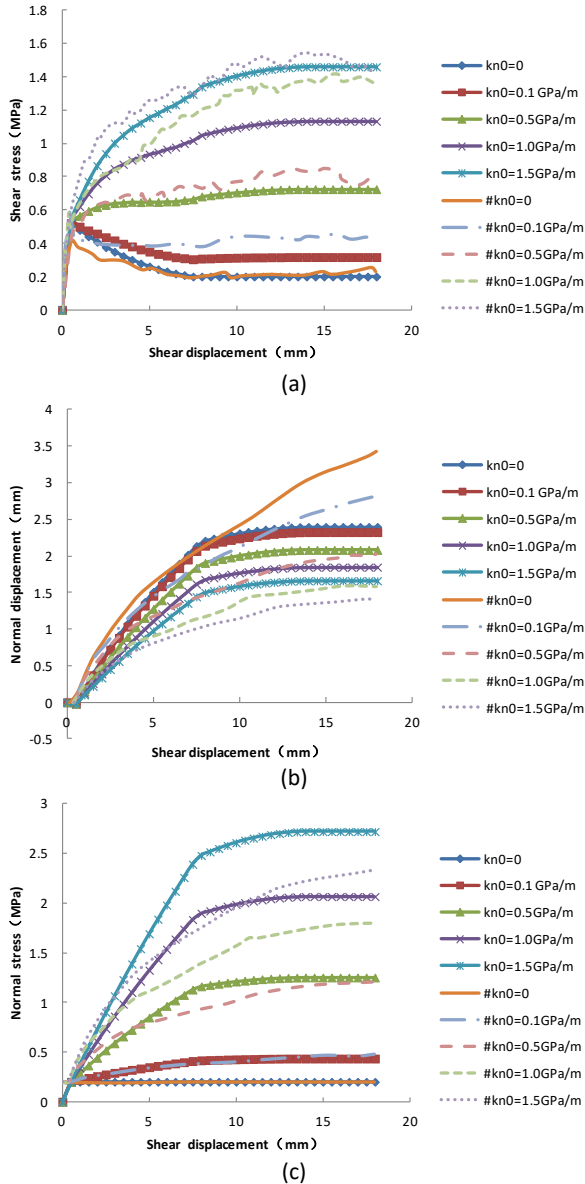


Figure 6 Comparison of complete shear stress-displacement curves between those by lab tests(Lee et al., 2014) and those by proposed approach under CNS condition, (a) shear stress-displacement curves, (b) normal displacement-shear displacement curves, (c) normal stress- shear displacement curves of a rock joint.

In Figure 6(b), normal displacement-shear displacement curves show that normal displacement will decrease as k_{n0} increases. As shown in Figure 6 (c), although the normal displacements decrease, the normal stress will increase as k_{n0} increases, which reveals that

the product of normal spring stiffness and normal displacement will increase as k_{n0} increases.

4.2 Shear behavior of rock joints with high normal spring stiffness

As the application of the presented method, shear behavior can be modeled with high normal spring stiffness on the basis of the Parameters in Table 1. The initial normal stress $\sigma_{n0}=2.5\text{MPa}$, but high normal stiffness k_{n0} ($=1.0, 10.0, 100.0$ and 1000.0GPa/m) is considered. Moreover, CND condition is taken into account.

Complete shear stress-displacement curves are presented in Figure 7.

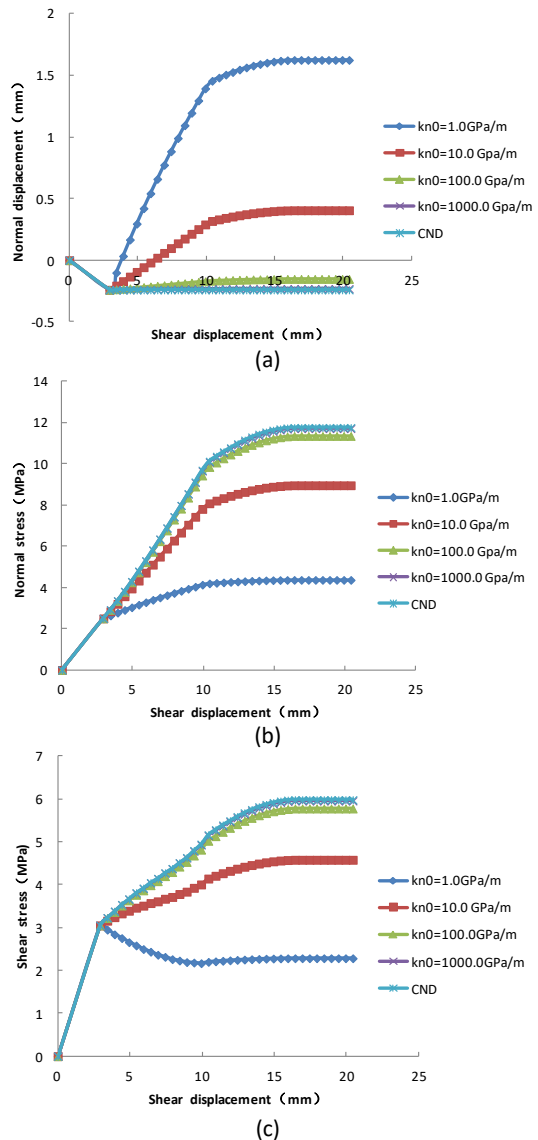


Figure 7 Shear behavior with high normal spring stiffness when the initial normal stress σ_{n0} equals to 2.5MPa, (a) normal displacement-shear displacement curves, (b) normal stress-shear displacement curves, (c) shear stress-displacement curves of the rock joint.

Figure 7(a) shows that the dilation quickly decreases as normal spring stiffness sharply increases. When k_{n0} is large enough, CNS condition changes into CND condition. In fact, when k_{n0} reaches 1000.0GPa/m, the dilation is restrained and the dilation can be ignored during shear process.

As shown in Figure 7(b), the normal stress increases with the increase of normal spring stiffness, and it reaches its maximum in CND condition. The main contribution of normal stress comes from the normal spring.

In Figure 7(c), the shear stress-displacement curve displays strength softening mode when k_{n0} equals to 1.0GPa/m, whereas it demonstrates a strength hardening mode when k_{n0} is larger than 10.0GPa/m.

In this case, the normal stiffness increases from 1.0GPa/m to 1000.0GPa/m. Obviously, the higher the normal stiffness is, the smaller the dilation is, and the higher the normal stress is. Meanwhile, the resistance to shear deformation is strong.

When the normal stiffness is large enough(for example, k_{n0} reaches 1000.0GPa/m), the dilation is almost completely restrained. The boundary condition is close to CND condition.

Comparing with the Figure 7, the complete shear stress-displacement curves are obtained in the same conditions only when the initial normal stress σ_{n0} changes into 5.0MPa, which is shown in Figure 8.

When the initial normal stress increases from 2.5MPa to 5.0MPa, the shear stress-displacement curve displays a complicated shear mode. It behaves as a strength softening mode when k_{n0} equals to 1.0GPa/m. While $k_{n0} \geq 10.0$ GPa/m, it shows a strength softening mode at first, but strength hardening mode follows as the shear deformation continues, as shown in Figure 8(c).

The normal displacement-shear displacement curves(Figure 8(a)) and the normal stress-shear displacement curves(Figure 8(b)) have the similar trends to those in Figure 7(a) and 7(b), respectively. The high normal stiffness restrains the dilation a lot, but it causes great increment of the normal stress.

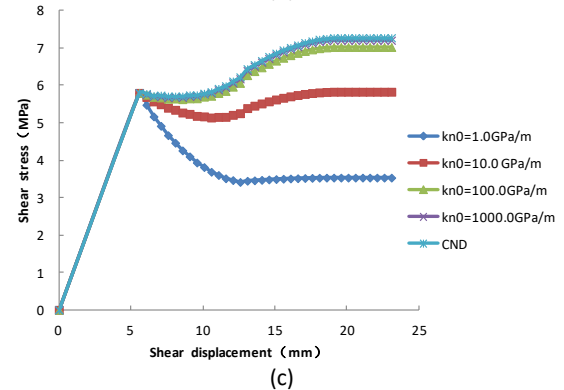
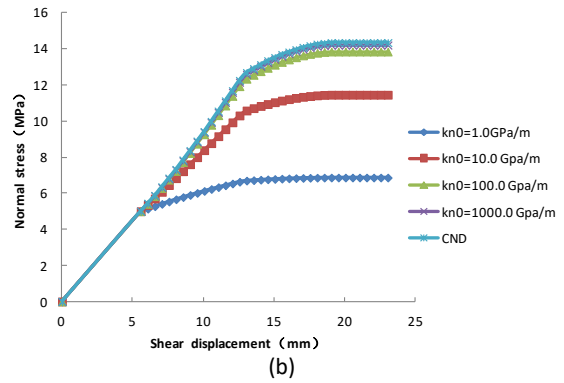
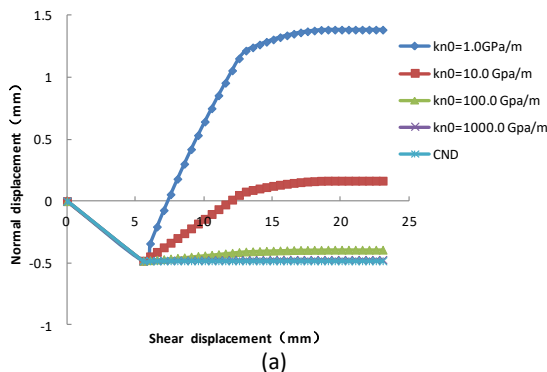


Figure 8 Shear behavior with high normal spring stiffness when the initial normal stress σ_{n0} equals to 5.0MPa, (a) normal displacement-shear displacement curves, (b) normal stress-shear displacement curves, (c) shear stress-displacement curves of the rock joint.

5 DISCUSSION AND CONCLUSION

In CNL condition, strength softening behavior is usually observed during shear deformation in rock joints. However, shear stress-displacement curve displays multiple modes in CNS condition, i.e. strength softening or strength hardening mode will probably appear under various CNS conditions.

With strength softening process treated as a series of stress drop and plastic flow, an improvement is made to model strength softening and strength hardening process in a unified form, and the numerical formulation is presented.

Shear behavior is studied under various CNS conditions. Both strength softening and strength hardening modes are modeled. The prediction of the overall shear behavior is consistent with the published test results. Comparisons indicate that the proposed approach is reliable.

Normally, the joint sliding causes dilation which acts against the rock mass surrounding underground caverns. The initial normal stress and normal stiffness of the surrounding rock mass would be high in caverns at great depth. Under these conditions, the normal stress is increased during joint sliding, and the dilation is restrained. The shear stress-displacement curves display a complicated mode. In some cases, the shear stress-

displacement curve displays partially a strength softening mode and partially a strength hardening mode.

On the basis of the theory of the plasticity, the proposed approach is efficient in modeling the shear behavior of rock joints. Moreover, the complicated shear behavior can be rationally predicted through numerical analysis by only using those basic parameters such as shear stiffness, normal stiffness, cohesion, friction angle, and dilatancy angle.

ACKNOWLEDGEMENTS

The authors thank China National Natural Science Foundation (Grant Nos. 41472289 & 51179185) and National Basic Research Program (Grant No. 2014CB047100) for supporting the work.

REFERENCES

- Bandis, S.C., Lumsden, A.C. and Barton, N. 1983. Fundamentals of rock joint deformation. *Int. J. Rock Mech. Sci. Geomech. Abstr.*, 20:249–68.
- Brady, B. H. G. and Brown, E. T. 2004. *Rock Mechanics for underground mining*. 3rd ed. Dordrecht: Springer Science.
- Goodman, R.E., Taylor, R. L. and Brekke, T.L. 1968. A model for the mechanics of jointed rock. *Journal of the Soil Mechanics and Foundations Division*. 94 (3) : 637-660.
- Grassellia, G. and Egger, P. 2003. Constitutive law for the shear strength of rock joints based on three-dimensional surface parameters, *International Journal of Rock Mechanics & Mining Sciences*, 40: 25–40.
- Indraratna, B., Haque, A. and Aziz, N. 1998. Laboratory modeling of shear behavior of soft joints under constant normal stiffness conditions. *Geotechnical and Geological Engineering*. 16: 17–44.
- Jiang, Y., Xiao, J., Tanabashi, Y. and Mizokami, T. 2004. Development of an automated servo-controlled direct shear apparatus applying a constant normal stiffness condition. *International Journal of Rock Mechanics and Mining Sciences*. 41: 275-286.
- Lee, Y.K., Park, J.W. and Song, J.J. 2014. Model for the shear behavior of rock joints under CNL and CNS conditions. *International Journal of Rock Mechanics and Mining Sciences*. 70: 252-263.
- Ohnishi, Y., Chan, T. and Jing, L. 1996. Constitutive models for rock joints. *Coupled Thermo-Hydro-Mechanical processes of fractured media, Developments in Geotechnical Engineering*. 79:57-22.
- Plesha, M.E. 1987. Constitutive models for rock discontinuities with dilatancy and surface degradation, *Int J Numer Anal Meth in Geomech*. 11:345-362.
- Wang, J.G., Ichikawa, Y. and Leung, C.F. 2003. A constitutive model for rock interfaces and joints. *International Journal of Rock Mechanics and Mining Sciences*. 40(1): 41-53.
- Wang, S.L., Guo, M.W. and Lu, Y.F. 2016. Study on shear-weakening behavior of rock joints. *the 69th Canadian Geotechnical Conference (GeoVancouver 2016)*, Vancouver, Canada
- Wang, S.L., Zheng, H., Li, C.G. and Ge, X. R. 2011. A finite element implementation of strain-softening rock mass. *International Journal of Rock Mechanics & Mining Sciences*. 48: 67-76.